OUKA

The University of Osaka
Institutional Knowledge Archive

State Analysis on Sulphur Ion in a Synthetic Blast Furnace Slag †

Nobuya IWAMOTO* and Yukio MAKINO**

Abstract

State of sulphur in synthetic blast furnace slag was investigated with visible-near infrared absorption, electron spin resonance and S K_α emission X-ray spectroscopy. Further, morphology of primary phase was observed with scanning electron microscope. Chemical shift in S K_α emission X-ray spectrum supported the result reported by Richardson et al. From the results of visible-near infrared absorption and electron spin resonance measurements, strong interaction between ferric and sulphur ions was indicated. However, further investigation is required for determination of the structure around iron. Morphology of primary phase, in most cases, was spherical though depending upon the additional form of sulphur. The clear relationship between partial oxygen pressure and morphology of primary phase could not be determined. Richness of sulphur was not always detected in primary phase, so that it can be considered that segragation of sulphur is not always effective to the crystallization of the slag.

1. Introduction

Slag is the essential material in iron- and steel-making and, in blast furnace refining, about 400 kg is produced in the production of 1 ton steel. Blast furnace slag has been utilized since sixteenth century and its main utilization at the present time is for civil engineering such as pavement and aggregate for concrete. In such utilization, however the most troublesome problem is the stench due to H_2S or yellow water originated from sulphur in slag. At present, it is difficult to say that the formation mechanism of yellow water is well-established although it has been considered that yellow water is attributed to calcium hypersulphide CaS_x which is formed as the result of the reaction of sulphide in slag with water or oxygen. When blast furnace slag is utilized for various purposes, such disadvantages are solved by the so-called "aging" method in which sulphur in slag is stabilized by preoxidation. There is another method in which sulphur is fixed by adding some stabilizer to molten slag. However, almost every methods on the stabilization of sulphur is under investigation.

Thus, various methods on stabilization of sulphur have been performed until now but there is no study in which the dissoluble property of sulphur in slag is connected with the state of sulphur. In this study, state of sulphur in synthetic blast furnace slag was investigated with several methods such as visible-near infrared (VIS-NIR) absorption, electron spin resonance (ESR) and emission X-ray spectroscopy. Further, morphology of primary phase was also investigated because the degree of crystallization in partial crystallized slag is very important to various utilization of slag.

2. Experimantal Procedures

The composition of parent synthetic blast furnace slag used is shown in **Table 1**. Glassy and partial crystallized

Table 1 Chemical composition of mother SBF slag.

CaO	SiO$_2$	MgO	Al$_2$O$_3$	FeO	CaO/SiO$_2$
42.88	35.00	5.46	15.98	0.35	1.225

slags were perpared by adding CaSO$_4$, CaS, elementary sulphur or K$_2$SO$_4$ to parent slag. Experimental conditions for producing each specimen slag are shown in **Table 2**. In order to determine state of sulphur in these

Table 2 Experimental conditions of specimen preparation.

Sample No.	Atomosphere	Temperature and Time	Addition	Mole%
1	$CO/CO_2=1/1$	1500°C (30min)	$CaSO_4$	3
2	$CO/CO_2=1/500$	1500°C (30min)	$CaSO_4$	3
3	$CO/CO_2=1/1$	1500°C (30min) → 1200°C (10min)	S	3
4	$CO/CO_2=1/500$	1500°C (30min) → 1200°C (10min)	S	3
5	$CO/CO_2=1/1$	1500°C (30min) → 1200°C (10min)	$CaSO_4$	3
6	$CO/CO_2=1/500$	1500°C (30min) → 1200°C (10min)	$CaSO_4$	3
7	in air	1500°C (30min) → 1200°C (10min)	S	3
8	in air	1500°C (30min) → 1200°C (10min)	S	5
9	in air	1500°C (30min) → 1200°C (10min)	CaS	5
10	$CO/CO_2=1/1$	1500°C (30min) → 1200°C (10min)	CaS	5
11	in air	1500°C (30min) → 1200°C (10min)	K_2SO_4	5
12	$CO/CO_2=1/1$	1500°C (30min) → 1200°C (10min)	K_2SO_4	5

specimen slags, ESR, VIS-NIR absorption spectra and chemical shifts in S K_α emission X-ray spectra were measured. These experimental conditions are as follows;

[Visible-Near Infrared Absorption]
  Range: 370 − 2600 nm,
  Specimen shape: Circular disk,
[S K_α emission X-ray study]
  Current and Voltage: 50kV × 40mA or 10mA,
  Crystal: Ge(111), Anticathode: Rh,
  Method: Fixed time (80 sec),
  Standard Material: S Powder,
[Electron Spin Resonance]
  Scan range: 0 − 5000 Gauss,
  Method: X-band,

Further, the observation with scanning electron microscope (SEM) was performed in order to examine the influence of sulphur addition on crystallization of synthetic blast furnace slag (SBF slag). The experimental conditions of SEM are as follows;

  Accelarating voltage: 20kV,
  Etchant: 5% nital or 10% $MgSO_4$ aq. sol.,
  Etching time: 2 − 5 min,
  Surface treatment: evaporated with Au.

3.   Results and Discussion

1) Chemical shift in S K_α emission X-ray spectrum in glassy SBF slag

These are many reports on sulphur in slag because of its importance in iron- and steel-making. Chemical and thermodynamical properties of sulphur in slag such as

solubility of sulphur or sulphide and activity of sulphide have been well investigated[1),2)] but state analysis on sulphur in slag has scarcely been performed until now. Fincham and Richardson investigated the dependency of sulphur in slag upon oxygen partial pressure (P_{O_2}) and presumed the state of sulphur by the approach based on thermodynamical equilibrium[3)]. According to their result, it is concluded that sulphur in slag is in the form of sulphide under the condition of $P_{O_2} < 10^{-6}$ atm whereas under the condition of $P_{O_2} > 10^{-4}$ atm, it is in the form of sulphate. Therefore, S K_α X-ray emission spectra of the SBF slags which were prepared in the CO/CO_2 mixed gas with the ratio 1/1 and 1/500, were measured in this study. There result are shown in **Fig. 1** and **Table 3**. As shown in Fig. 1, the peak of S K_α spectrum in the slag

Table 3 Chemical shifts in S K_α emission spectra of SBF slags.

Specimen No.	Peak Position of S K_α (°2ϑ)	$\triangle$°2ϑ	Half Width(deg.)
1	110.691	0.013	0.44
2	110.626	−0.052	0.50
3	110.692	0.014	0.45
4	110.689	0.011	0.40
5	110.703	0.005	0.48
6	110.683	0.025	0.44
$CaSO_4$	110.593	−0.085	0.39
S Powder	110.678	0.00	0.41

prepared in the CO/CO_2 mixed gas with 1/1 ratio (No.1 slag in Table 1) was found to occupy the similar position
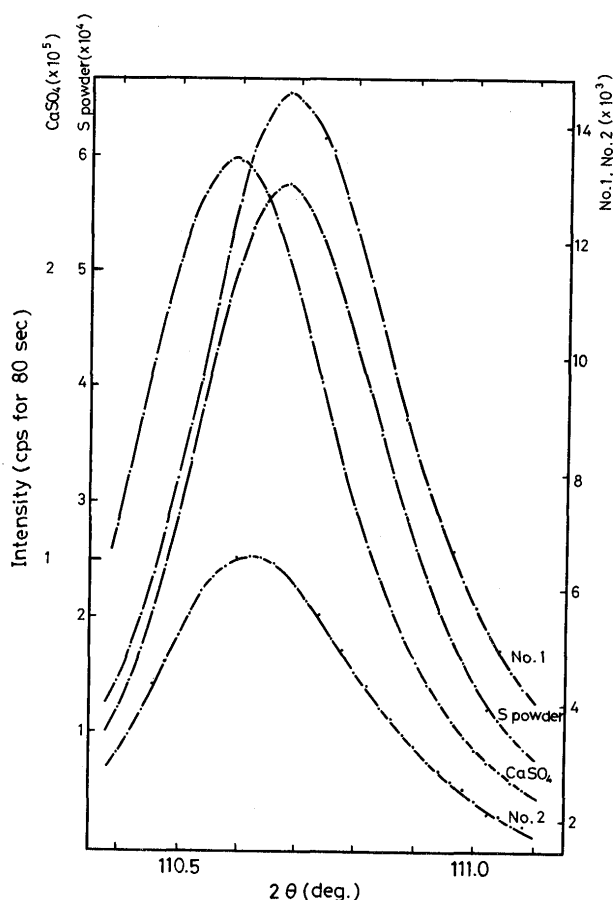
Fig. 1 S K_α emission spectra of glassy SBF slags.

to that obtained from elementary sulphur whereas the peak of the slag produced in the CO/CO_2 mixed gas with 1/500 ratio (No.2 slag in Table 1) was detected in the neighbourhood of the peak position of $CaSO_4$. This suggests that sulphur exists in the form of S^{2-} in a strong reducing condition and does in the form of SO_4^{2-} in a weak reducing condition. However, there are some room to discuss our result because elementary sulphur instead of a sulphide, for example CaS, was used as the standard material.

2) VIS-NIR absorption and ESR in glassy SBF slag

It is well known that strong interaction between iron and sulphur is often found out in silicate minerals[4]. Therefore, the dependency of the interaction between iron and sulphur in SBF slag upon P_{O_2} was investigated with VIS-NIR absorption and ESR methods. In other words, state of sulphur was indirectly investigated by identification of the state of iron ion. As shown in Fig. 2, the peak due to Fe^{2+} ion in octahedral site was detected in the neighbourhood of 10^4 cm^{-1} in both parent slags which were prepared in the strong and weak reducing conditions (see Table 2). However, the clear difference was found out in the slags with 3 mole% $CaSO_4$ prepared under the same conditions. That is, near-infrared absorp-

tion due to Fe^{2+} ion in octahedral site disappeared in the weak reducing condition in which CO/CO_2 ratio is 1/500. It can be considered that the disappearance is originated in (a) the change of crystal field around iron or (b) in the change of divalent iron ion to trivalent one by the addition of $CaSO_4$. However, conclusive decision can not be given from only the result of VIS-NIR absorption.
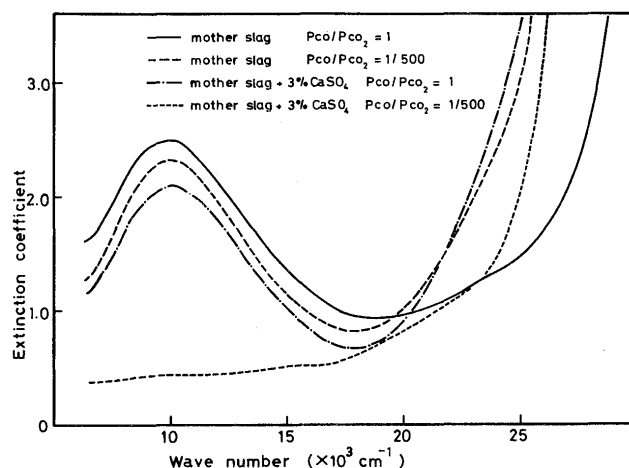

Fig. 2 Absorption spectra of SBF slags in visible and near infrared regions.

Subsequently, ESR measurement was performed to determine the precise state of iron ion in slag because ESR spectroscopy can detect the symmetry around the noticed ion. As shown in Table 4, ESR absorption was observed

Table 4 The values of peak positions in VIS-NIR absorption and ESR spectra.

	$CO/CO_2=1/1$ (No.1)		$CO/CO_2=1/500$ (No.2)	
Sulphur	without	added	without	added
VIS-NIR Absorption	$\cong 10^4$cm^{-1}	none	$\cong 10^4$cm^{-1}	$\cong 10^4$cm^{-1}
ESR	none	$\cong 1500$G	none	none

near 1500 gauss (g =4.3) only in the slag with 3 mole% $CaSO_4$ which was prepared in the CO/CO_2 mixed gas with the ratio 1/500. According to Tucker[5] and Hirayama et al.[6], the absorption with g = 4.3 originates from the group $Fe^{3+}O_4$. On the contrary, Kurkjian and Sigetity reported that it can not be determined whether the absorption with g = 4.3 is attributed to $Fe^{3+}O_4$ group or to $Fe^{3+}O_6$ group[7]. Likewise, Loveridge and Parke discussed the ESR spectra of iron ion in glass on the basis of group theory. He indicated that the spectrum with g = 4.3 originates from ion groups such as MA_2B_2, MA_3B_3

and MA_4B_2 which belong to C_{2v} symmetry group (M: cation such as Fe^{3+}, A, B: anions)[8]. Taking an example, ion groups with different symmetry such as $Fe^{3+}O^0O_3^-$, $Fe^{3+}O_2^0O_2^-$ can be considered even in $Fe^{3+}O_4$ group coordinated with different oxygen species. Besides, modifier cations in the second nearest neighbour can change the symmetry around noticed cation. Therefore, it can be considered that the absorption with g=4.3 is not due to only $Fe^{3+}O_4$ group. In amber glasses, some investigators suggested that absorption with g=4.3 can be attributed to $Fe^{3+}O_2S_2$ and absorption with g=6 originates from $Fe^{3+}O_3S$ and $Fe^{3+}OS_3$, so that it may be reasonable to interpret that ion groups of $Fe^{3+}O_{6-x}S_x$ produce absorption with g=4.3 because the existence of $Fe^{2+}O_6$ group was certified in the slag without $CaSO_4$. Further, the number of sulphur exchanged with oxygen would be two at most because sulphur content was 3 mole% or less. Therefore, possible iron groups would be $Fe^{3+}O_3S$, $Fe^{3+}O_2S_2$ and $Fe^{3+}O_4S_2$. In order to certify the discussion described above, however, further investigation is desired because only a few slag were investigated with ESR spectroscopy.

3) Chemical shift of S K_α emission X-ray spectrum in partial crystallized SBF slag

In order to examine whether the state of sulphur in SBF slag is changed by partial crystallization, chemical shift of S K_α emission X-ray spectrum in partial crystallized SBF slag was measured. As shown in **Fig. 3**, all peaks of S K_α spectra showed similar values to that in elementary sulphur. This does not always suggest that sulphur in partial crystallized SBF slag exists in the form of S^{2-} ion. However, it would be reasonable to interpret that the sulphur in partial crystallized SBF slags is in the form of S^{2-} because these chemical shifts were similar one to sample (2) and were fairly different from the value obtained from pure $CaSO_4$. Conclusively, sulphur ion in partial crystallized SBF slags does not exist in the from of SO_4^{2-} ion. It is difficult to explain the phenomenon on account of the insufficient data. However following explanation can be considered as one of these reasons. At 1500°C, CO/CO_2 mixed gas with the ratio 1/500 gives oxygen partial pressure of about 10^{-3} atm whereas P_{O_2} in the same mixed gas becomes 10^{-6} atm at 1200°C. Therefore, SBF slags are practically exposed to the atmosphere with $P_{O_2} = 10^{-6}$ atm during crystallizing at 1200°C, so that sulphate ion becomes unstabilized. However, many other causes can be considered on the unstabilization of sulphate ion. Therefore, further investigation on sulphur state with another method such as ESR is desired.

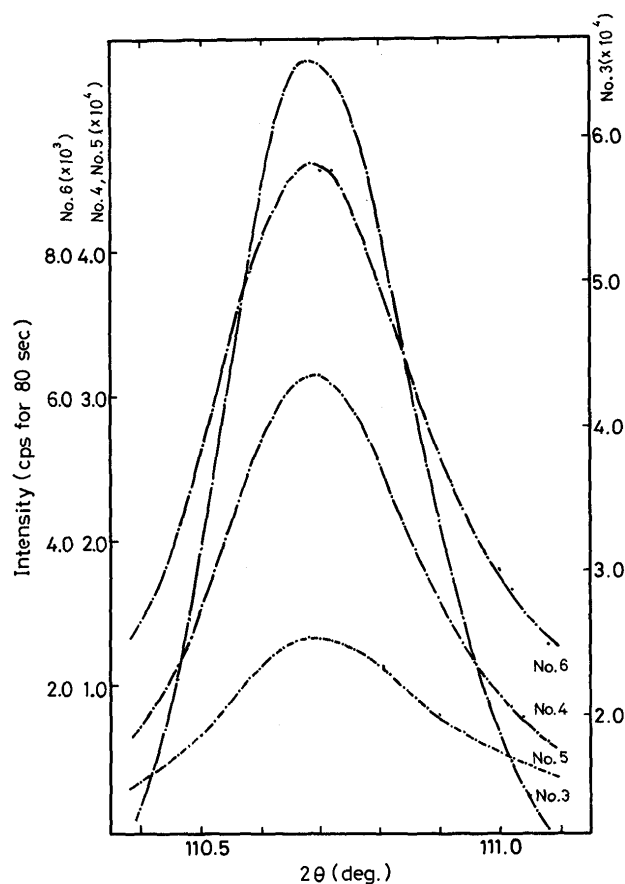4) Morphology of primary phase and segregation of sulphur in partial crystallized SBF slag

Fig. 3 S K_α emission spectra of partial crystallized SBF slags.

It is well known that slag is more easily crystallized by addition of sulphur. Hence, the influence of sulphur addition on the precipitation of primary phase was investigated by SEM observation and X-ray microanalysis. The addition of sulphur to SBF slag was performed in various forms such as CaS, $CaSO_4$, K_2SO_4 and elementary sulphur. Further the dependency of morphology of primary phase upon P_{O_2} was investigated under the limited conditions of $P_{O_2} = 10^{-8}$, 10^{-3} and 0.21. The result of SEM observation is shown in **Photo. 1** and **Table 5**. As shown in the result, morphologies of primary phases were, in most cases, spherical irrespective of the additional form of sulphur. In the specimens No.7, No.8 and No.10, primary phase precipitated in fairly complicated forms (named earthworm-like). Thus, morphology of primary phase, though not strictly, was spherical or earthworm-like.
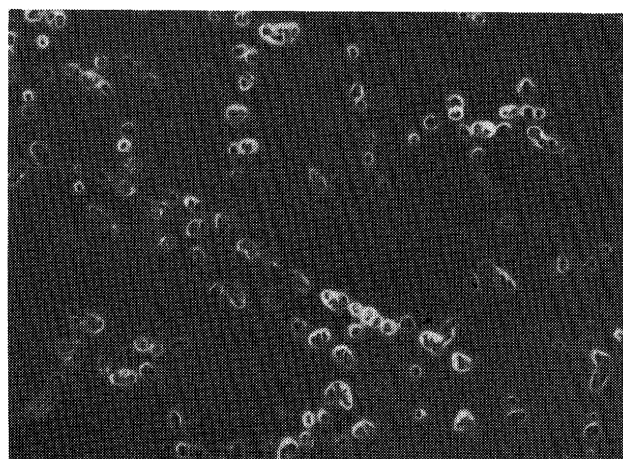
Subsepuently, the segregation of sulphur was examined with X-ray microanalysis. As shown in Table 5, the segregation of sulphur in primary phases was not always detected, so that it is concluded that the piling-up of sulphur not always enhances the precipitation of primary phase. These primary phases were identified as melilite
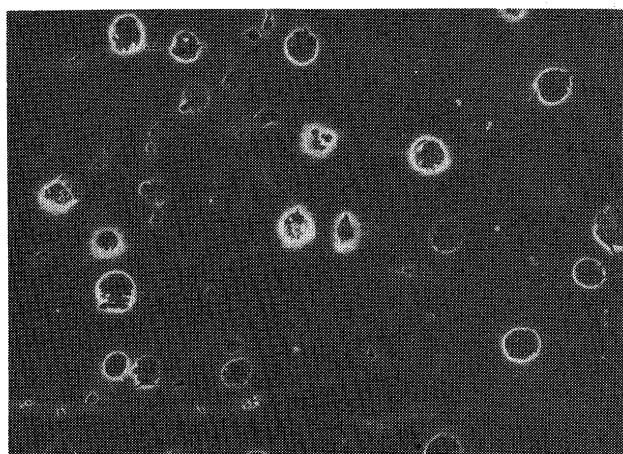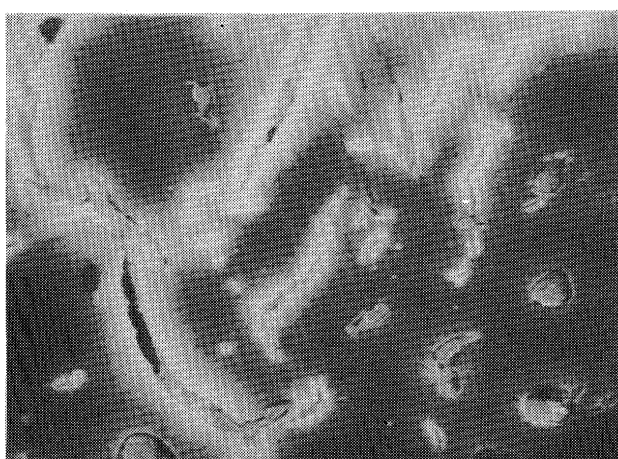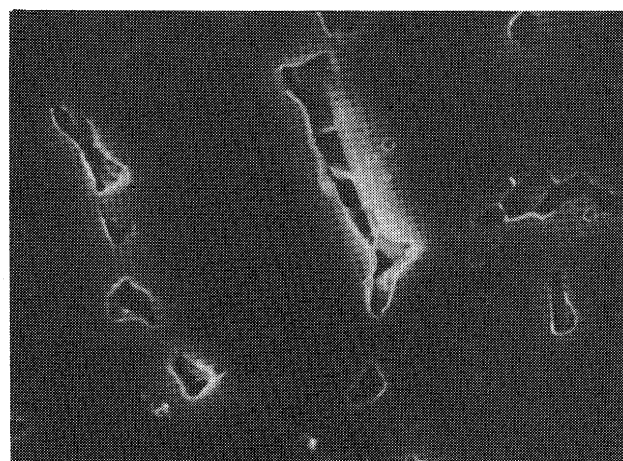
(a)
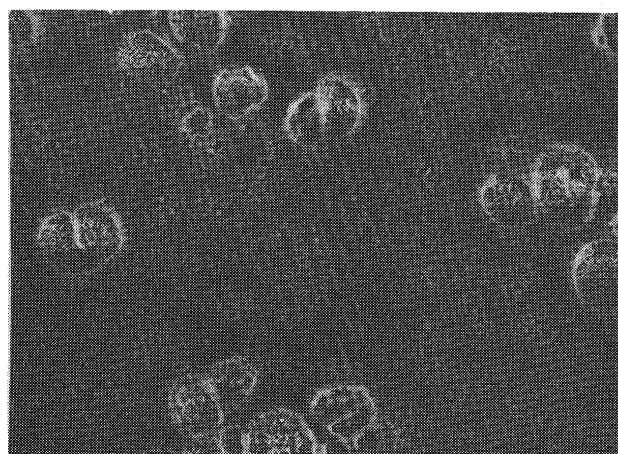
(b)

(c)

(d)

(e)

Photo. 1 Typical primary phases in several partial crystallized SBF slags.

(a) Specimen No.6 (×800),
(b) Specimen No.12 (×300),
(c) Specimen No.4 (×500),
(d) Specimen No.7 (×800),
(e) Partial crystallized parent SBF slag (×3000)
    [1500°C (30min)→1200°C (10min)]

from X-ray diffraction measurement. However, detailed study on the identification of primary phase is required because cystallization behaviour in SBF slag is very complicated. Further, the complication produces many difficulties for clear explanation on the relation among segregation of sulphur, Po_2 and morphology of primary phase. Therefore, it is also necessary to investigate the effects of sulphur addition on precipitation behaviour in simple slag.

Table 5 Morphology of primary phase and segregation of
sulphur in partial crystallized SBF slags

Addition / Atomosphere	CaSO₄	S Powder	CaS	K₂SO₄
air		sulphur rich in matrix earthworm-like	spherical (only isolated precipitate) sulphur rich in matrix (except precipitate near crucible wall)	spherical intra-segragation in precipitate
CO/CO₂=1/500	spherical sulphur rich in primary phase	spherical no difference between precipitate and matrix	——————	——————
CO/CO₂=1/1	spherical sulphur rich in precipitate	almost spherical no detectable	earthworm-like or seaweed-like criented precipitation pattern in well crystallized region	spherical and small island-like no remarkable differ- ence between precip- tate and matrix

4. Summary

In order to clarify effects of sulphur addition on crystallization in blast furnace slag, state of sulphur in SBF slag was investigated with VIS-NIR absorption, ESR and S K_α emission spectroscopy. Form these results, it was concluded that sulphur exists in the form of sulphide under the condition of $P_{o_2} = 10^{-6}$ atm or less whereas it is in the form of sulphate under the condition of $P_{o_2} = 10^{-4}$ atm or over as indicated by Fincham and Richardson. Further, possible structures around iron ion were discussed from the result of ESR. Morphology of primary phase was also investigated with SEM and X-ray micro-analysis. SEM observation showed that primary phase was detected, though roughly, in the spherical or earthworm-like form. The relationship betwee P_{o_2} and morphology of primary phase could not be determined clearly. Richness of sulphur was not always detected in primary phase. Therefore, the crystallization in SBF slag is not always enhanced by the segregation of sulphur.

Acknowledgement

References

1) F. D. Richardson: "Physical Chemistry of Melts in Metallurgy", Vol.2, Chap.8, Academic Press, (1974).
2) for example; R. A. Sharma and F. D. Richardson: Trans. Met. Soc. AIME, 233 (1965),p.1586.
3) C. J. B. Fincham and F. D. Richardson: Proc. Roy. Soc. London, A223, (1954), p.40.
4) J. W. D. Connolly and D. R. Haughton: Amer. Mineral., 57 (2972), p.1515.
5) R. F. Tucker: "Advances in Glass Technology", p.103, (1962), Plenum Press, New York.
6) C. Hirayama, J. G. Castle and M. Kuriyama: Phys. Chem. Glasses, 9 (1968), p.109.
7) Kurkuian and E. A. Siegety: Phys. Chem. Glasses, 9 (1968), p.73.
8) D. Loveridge and S. Parke: Phys. Chem. Glasses, 12 (1971), p.19.